Science of the Total Environment 619–620 (2018) 1163–1169

Contents lists available at ScienceDirect

Science of the Total Environment

journal homepage: www.elsevier.com/locate/scitotenv

Emission characteristics of atmospheric carbon dioxide in Xi'an, China based on the measurements of CO_2 concentration, $\Delta^{14}C$ and $\delta^{13}C$

Peng Wang [a,b,c], Weijian Zhou [a,b,d,*], Zhenchuan Niu [a,b], Peng Cheng [a,b], Shugang Wu [a,b], Xiaohu Xiong [a,b], Xuefeng Lu [a,b], Hua Du [a,b]

[a] State Key Laboratory of Loess and Quaternary Geology, Institute of Earth Environment, Chinese Academy of Sciences, Xi'an, China
[b] Shaanxi Provincial Key Laboratory of Accelerator Mass Spectrometry Technology and Application, Xi'an AMS Center, Xi'an, China
[c] University of Chinese Academy of Sciences, Beijing, China
[d] Beijing Normal University, Joint Center For Global Changes Studies (JCGCS), Beijing, China

HIGHLIGHTS

- Atmospheric CO_2, as well as $\Delta^{14}C$ and $\delta^{13}C$ were observed regularly in Xi'an.
- Urban CO_2 "dome" effect was particularly evident during winter season.
- Average contribution of CO_{2ff} in winter were lower than that in summer.
- Coal burning was the dominant source of fossil fuel emissions in winter.
- Biogenic activities play an important role in urban carbon cycles.

GRAPHICAL ABSTRACT

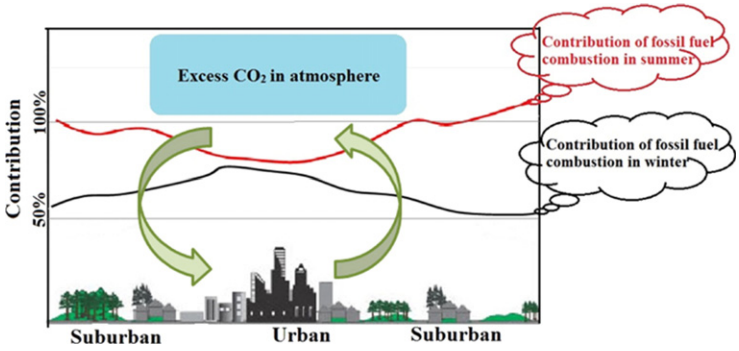

ARTICLE INFO

Article history:
Received 5 October 2017
Received in revised form 10 November 2017
Accepted 10 November 2017
Available online 29 November 2017

Editor: Xuexi Tie

Keywords:
Atmospheric CO_2
$\Delta^{14}C$
$\delta^{13}C$
Sources and sinks

ABSTRACT

Given that cities contributed most of China's CO_2 emissions, understanding the emission characteristics of urban atmospheric CO_2 is critical for regulating CO_2 emissions. Regular observations of atmospheric CO_2 concentration, $\Delta^{14}C$ and $\delta^{13}C$ values were performed at four different sites in Xi'an, China in 2016 to illustrate the temporal and spatial variations of CO_2 emissions and recognize their sources and sinks in urban carbon cycles. We found seasonal variations in CO_2 concentration and $\delta^{13}C$ values, the peak to peak amplitude of which was 80.8 ppm for CO_2 concentration and 4.0‰ for its $\delta^{13}C$. With regard to the spatial variations, the urban CO_2 "dome" effect was the most pronounced during the winter season. The use of $\Delta^{14}C$ combines with $\delta^{13}C$ measurements aid in understanding the emission patterns. The results show that in the winter season, emissions from fossil fuel derived CO_2 (CO_{2ff}) contributed 61.8 ± 10.6% and 57.4 ± 9.7% of the excess CO_2 (CO_{2ex}) in urban and suburban areas respectively. Combining with the result of estimated $\delta^{13}C$ value of fossil fuel ($\delta^{13}C_{ff} = -24‰$), which suggest coal burning was the dominant source of fossil fuel emissions. In contrast, the proportions of CO_{2ff} in CO_{2ex} varied more in the summer season than that in the winter season, ranging from 42.3% to >100% with the average contributions of 82.5 ± 23.8% and 90.0 ± 24.8%. Given the estimation of $\delta^{13}C$ value of local sources ($\delta^{13}C_s$) was −21.9‰ indicates that the intensively biogenic activities, such as soil respiration and corn growth have significantly impacted urban carbon cycles, and occasionally played a role of carbon sink.

* Corresponding author at: State Key Laboratory of Loess and Quaternary Geology, Institute of Earth Environment, Chinese Academy of Sciences, Xi'an, China.
E-mail address: weijian@loess.llqg.ac.cn (W. Zhou).

http://dx.doi.org/10.1016/j.scitotenv.2017.11.125
0048-9697/

1. Introduction

Carbon dioxide (CO_2) is one of the most important anthropogenic greenhouse gas, the global average CO_2 concentration has reached 400 ppm in 2015, with the mean annual absolute growth of 2 ppm during the last decade (WMO, 2016). Emissions from fossil fuel combustion are the primary driver of this increase (Ballantyne et al., 2015). Therefore, quantifying the emissions of fossil fuel CO_2 (CO_{2ff}) is essential for regulations to reduce CO_2 emissions thereby mitigate the effects of global climate change as well as implement low carbon development strategies (Duren and Miller, 2012).

The most common method to estimate CO_{2ff} emissions is through bottom-up inventory data, which uses the energy activity data and relevant fossil fuel emission factors to estimate CO_{2ff} emissions (IPCC, 2006). This method provides useful information toward the determination of CO_{2ff} emission levels at national or regional scales and helps to define emission reduction goals. However, due to inconsistencies of statistical data and differences in the estimated emission factors, uncertainties vary between 3% and 40% at the national scale on annual estimate (Marland et al., 2009), and the uncertainties will increase with the decrease in spatial scale (Gurney et al., 2009). Furthermore, since the availability of energy consumption data for most cities in China is limited (Liu et al., 2012) and it's difficult to define a city's boundary for CO_{2ff} emissions accounting (Liang and Zhang, 2011), so there are some challenges to use bottom-up method for city's CO_{2ff} emissions research.

As CO_2 emissions become regulated and the needs of verifying reductions, it is necessary to seek other methodologies to achieve more satisfactory results (Tans and Wallace, 1999). "Top-down" atmospheric measurements have been proposed to independently evaluate CO_{2ff} emissions and as a complement to the widely used bottom-up method (Ciais et al., 2010; McKaina et al., 2012). A number of studies have shown that radiocarbon (^{14}C) content analysis on air samples is a highly effective atmospheric top-down proxy for quantifying CO_{2ff} components and biogenic CO_2 sources at different spatial and temporal scales (Levin et al., 2003; Turnbull et al., 2006). Because fossil fuels are made of sedimentary organic matter that is much older than the half-life of ^{14}C (5730 $\pm$ 40 years) (Godwin, 1962), their ^{14}C content has decayed to undetectable level in fossil fuels, and causing a decrease in the ratio of $^{14}C/^{12}C$ when CO_{2ff} is persistently released into the atmosphere (Suess, 1955). Thus, it is possible to quantify the fractions of CO_{2ff} emission by measuring the ratio of $^{14}C/^{12}C$ in atmosphere. The stable carbon isotopic composition ($\delta^{13}C$) can be used to constrain CO_{2ff} sources further due to distinct isotopic signatures between fossil fuel and biogenic sources. Such as the $\delta^{13}C$ value of natural gas typically being lower than that of petroleum (Ballantyne et al., 2011; Djuricin et al., 2010; Newman et al., 2016; Pataki et al., 2003a; Widory and Javoy, 2003).

Being hot spots for anthropogenic CO_2 emissions, cities contribute about three-quarters of global CO_{2ff} emissions within a small fraction of the total land area on earth (IEA, 2008; Seto et al., 2014). In China in particular, emissions from cities' energy usage were estimated to contribute ~85% of China's CO_2 emissions (Dhakal, 2009, 2010). Therefore, using a top-down approach to quantitatively understand the sources and magnitude of cities CO_2 emissions in China is a key scientific issue in carbon emission-reduction research. This requires including not only the measurements of atmospheric CO_2 concentrations in cities, but also the identification of their sources and sinks, as well as quantifying their relative contributions, especially for CO_{2ff} emissions. These are considered as important steps toward addressing the challenge of greenhouse gas mitigation (Newman et al., 2016).

To this end, atmospheric CO_2 concentrations and $\delta^{13}C$ values were observed regularly from the January to the November of 2016 at four sites in Xi'an city, and $\Delta^{14}C$ in the winter and summer seasons were also measured. We attempt to (1) present the spatial and temporal characteristics of the urban atmospheric CO_2 concentration and $\delta^{13}C$; (2) quantify the contributions of anthropogenic and biogenic emissions in different regions and seasons of the city; and (3) make a qualitative analysis of the dominant source of fossil fuel and biogenic emission in urban carbon cycles.

2. Materials and methods

2.1. Sampling sites

Xi'an is located in the Guanzhong Plain (Fig. 1 left) and is the biggest city in west China, with a population of nearly 8.7 million in 2016. The city is sandwiched between the Loess Plateau in the north and the QinLing Mountains in the south. Xi'an has an average elevation of 400 m a.s.l and an annual precipitation of 553 mm, this city is influenced by the East Asian monsoon system with a character of semi-humid condition, and the monthly average temperature ranges from around the freezing mark in December to 29.0 °C in July (Xi'an Municipal Bureau of Statistics, 2016). Atmospheric air samples were collected at 4 sites, distributed over different regions of the city (Fig.1 right). Sampling sites A and B are the two urban area sites, which were located in Taibai Campus of Northwest University and Weishi Street, respectively. C and D sites represent the two suburban locations within Han Chang 'an ruins zone and High-tech industrial zone, respectively. All of these sites are located more than 200 m from any main roads and were assumed not influenced by local traffic and other environmental factors.

The Waliguan (WLG) Global Atmosphere Watch (GAW) station (36.28° N, 100.9° E) is the only inland atmospheric background station on the Eurasian continent and is located at the highest altitude (3816 m a.s.l.) in the world. It is located on the northeast slope of the Qinghai-Tibet plateau in western China (Fig. 1 left), and it is rarely influenced by human activities. As such, it was selected as a background site for this study.

2.2. Sample collection

Sampling campaigns were carried out at one week intervals, and all sampling was conducted on the same day of the week and typically near 14:00 of local time, when the planetary boundary layer (PBL) tends to be deepest and air is well mixed during the day (Newman et al., 2016). So the isotopic signature is expected to reflect the average level of local sources, though the diurnal CO_2 concentrations tend to be low level during the day (Idso et al., 2001; Necki et al., 2003). All air samples were collected with a pump to fill a 5-L aluminum foil air bag (Delin Gas Packing Co., Ltd. Dalian, China) for 10–15 min. Before sampling, each bag was evacuated to approximately 10^{-2} mbar in a pretreatment lab and purged with ambient air at the sampling site for 3 min in order to displace any remaining gas. After the completion of air sampling, air bags were transported to the laboratory for further analysis. The sampling was done once a week over a period of 11 months. In some weeks, the sampling was not conducted due to inclement weather and other issues. A total of 150 air samples from all four sites were collected for the determination of CO_2 concentration and $\delta^{13}C$, and 75 air samples, which collected during winter and summer seasons were conducted for ^{14}C isotopic analyses.

2.3. Sample preparation and measurements

All air samples were first measured using a Picarro G2131-I CO_2 Isotopic Analyzer (Picarro Inc., USA). The instrument is based on cavity ring down spectroscopy (CRDS), with the cap abilities of high precision, linearity and stability for CO_2 measurement (Crosson, 2008). Each sample was measured for approximately 6 min and the measurement frequency was 1 s. Only the average value of the last 4 min for each sample was used in order to reduce the uncertainties, and CO_2 concentrations were determined by summing the $^{12}CO_{2dry}$ and $^{13}CO_{2dry}$ data. The standard reference gases were obtained from Chinese Academy of Meteorological Science, their concentration and $\delta^{13}C$ values were traceable to the

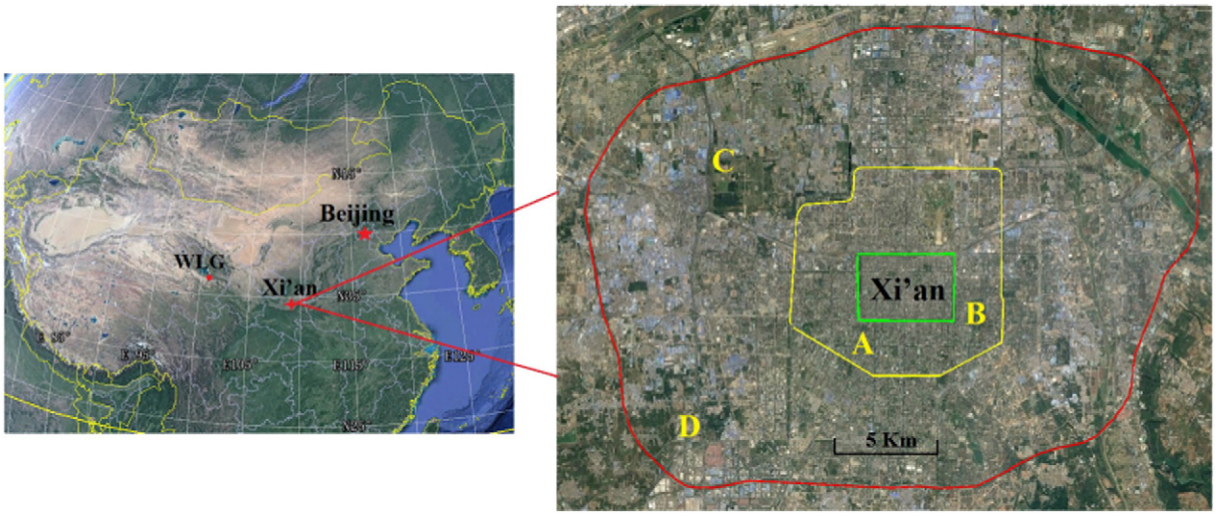

Fig. 1. The location of Xi'an city within China and the detailed location of the sampling sites in Xi'an. The colorful circles on the right panel represent the loop road and the expressway in Xi'an city, respectively.

Central Calibration Laboratory(CCL)of WMO (World Meteorological Organization) 2007 scale and NBS-19 and NBS-20 standard reference materials of NOAA-ESAL, respectively. The values of $\delta^{13}C$ are expressed relative to the Vienna Pee Dee Belemnite (VPDB) standard (Coplen, 1996).

$$\delta^{13}C = \left(R_{sample}/R_{s\ tandard} - 1\right) \times 1000‰ \quad (1)$$

R is the ratio of heavy carbon (^{13}C) isotope to light carbon (^{12}C) isotope.

After the completion of CO_2 measurements, the residual samples collected in winter and summer were allowed to flow through a vacuum system at a rate of 200 mL/min (Zhou et al., 2014).The air passed through a liquid nitrogen cold trap (−196 °C) to freeze CO_2 and water, then the water was removed by an ethanol-liquid nitrogen cold trap (−90 °C), and the CO_2 was purified (Zhou et al., 2014). The purified CO_2 was reduced to graphite using the zinc iron method, in which zinc power is used as a reductant and iron as a catalyst (Jull, 2007; Slota et al., 1987).

The graphite was then pressed into an aluminum holder and ^{14}C was measured using a 3 MV accelerator mass spectrometer (AMS) in Xi'an, China, with a precision of 2‰ measurement (Zhou et al., 2006). The results can be reported as $\Delta^{14}C$, which is the per mil (‰) deviation from the absolute radiocarbon standard and is corrected by the international common method (Stuiver and Polach, 1977).

$$\Delta^{14}C = \left[\frac{\left(^{14}C/^{12}C\right)_{SN}}{\left(^{14}C/^{12}C\right)_{ABS}} - 1\right] \times 1000‰ \quad (2)$$

Here, $(^{14}C/^{12}C)_{SN}$ is the atomic ratio of $^{14}C/^{12}C$ in the sample which is normalized to a $\delta^{13}C$ of −25‰, and $(^{14}C/^{12}C)_{ABS}$ is the absolute radiocarbon reference standard.

2.4. Calculation

2.4.1. Calculation of CO_{2ff} based on $\Delta^{14}C$

In general, the major sources of atmospheric CO_2 (CO_{2obs}) can be divided into three components: fossil fuel CO2 (CO_{2ff}), biogenic emission (CO_{2bio}) and the atmospheric background (CO_{2bg}). The $\Delta^{14}C$ values of these components are expressed as Δ_{obs}, Δ_{ff}, Δ_{bio}, and Δ_{bg}, respectively. According to two mass balance equations of CO_2 concentrations and $\Delta^{14}C$ (Levin et al., 2003; Miller et al., 2012; Pataki et al., 2003a; Turnbull et al., 2006; Zimnoch et al., 2012), the following equations can be written:

$$CO_{2obs} = CO_{2ff} + CO_{2bg} + CO_{2bio} \quad (3)$$

$$\Delta_{obs}CO_{2obs} = \Delta_{ff}CO_{2ff} + \Delta_{bg}CO_{2bg} + \Delta_{bio}CO_{2bio} \quad (4)$$

Then, rearranging Eq. 3 and Eq. 4, CO_{2ff} can be calculated as follows:

$$CO_{2ff} = \frac{CO_{2obs}\left(\Delta_{obs} - \Delta_{bg}\right)}{\Delta_{ff} - \Delta_{bg}} - \frac{CO_{2bio}\left(\Delta_{bio} - \Delta_{bg}\right)}{\Delta_{ff} - \Delta_{bg}} \quad (5)$$

In Eq. (5), $\Delta_{ff} = -1000‰$, and the second term of the right – hand side in the Eq. (5) is the bias (β) term. In general, Δ_{bio} is assumed to be equal to Δ_{bg} because autotrophic respiration is considered to be the main source of biosphere (Levin et al., 2003). If β is ignored, CO_{2ff} would be underestimated by 0.4–0.8 ppm in summer and 0.2–0.3 ppm in winter (Hsueh et al., 2007; Palstra et al., 2008; Riley et al., 2008; Turnbull et al., 2009; Turnbull et al., 2006). Specifically, in most temperate Northern Hemisphere regions, the effect of this term underestimates CO_{2ff} by 0.2 ppm in winter and 0.5 ppm in summer (Turnbull et al., 2009), which were used to correct CO_{2ff} in this study.

The choice of atmospheric background $\Delta^{14}C$ can influence the estimate of the CO_{2ff} concentrations. In general, an ideal background site should be located in the free troposphere, but it's difficult for a long-term observation, and therefore high altitude mountains are usually selected as proxies of free troposphere background sites (Turnbull et al., 2009). In this study, we selected WLG as the background site and the average $\Delta^{14}C$ value of 17.1 ± 6.8‰ was reported in 2015 (Niu et al., 2016). Because there is no background $\Delta^{14}C$ values were available for 2016, we used the value of 12.1‰ as the annual background $\Delta^{14}C$ value of 2016 in this study which were inferred based on the annual decline of approximately 5‰ at Pt. Barrow, AK in recent years (Graven et al., 2012). According to our measurement data, there is a bias of about 0.4 ppm for CO_{2ff} when the change of background $\Delta^{14}C$ value is 1‰.

2.4.2. Determination of $\delta^{13}C$ signature of the local CO_2 sources

There are two methods to determine the $\delta^{13}C$ signature of the local source ($\delta^{13}C_s$), such as from the Keeling plot (Keeling, 1958) and from the Miller-Tans plot (Miller and Tans, 2003). Both methods have their certain assumptions, for example, the basic assumption of Keeling plot method is that only two gas components are considered and their isotopic compositions do not change during the observation period (Pataki et al., 2003b). The Miller-Tans approach requires a record of the

background CO_2 concentrations and $\delta^{13}C$ but the Keeling plot method does not. Although (Zobitz et al., 2006) have found that there were not inherent advantage or disadvantage between these two methods, Keeling plot method is generally used for samples collected at nighttime or winter season when sinks and sources do not occur simultaneously (Vardag et al., 2016). Thus the Miller-Tans plot method was chosen to determine the local CO_2 source signature as follows:

$$\delta^{13}C_{obs}C_{obs} = \delta^{13}C_s(C_{obs} - C_{bg}) + \delta^{13}C_{bg}C_{bg} \quad (6)$$

In linear Eq. (6), when $\delta^{13}C_sC_{obs}$ is plotted in the y-axis and $\delta^{13}C_{bg}C_{bg}$ is plotted in x-axis, then, the isotopic composition of the local source ($\delta^{13}C_s$) is the slope of this line, which is determined by Model I (ordinary least squared) regression technique (Zobitz et al., 2006). The value of $\delta^{13}C_s$ represents the flux-weighted mean isotopic composition of the local CO_{2ff} sources, including anthropogenic and biogenic sources during the observation period (Miller and Tans, 2003). In theory, $\delta^{13}C_s$ should range from the end member of C_4-type ecosystems to natural gas.

In this study, the observed data of WLG in 2016 was used as the background CO_2 concentrations in our observation period. Because of the unavailability of $\delta^{13}C$ data for the time interval of interest, the background $\delta^{13}C$ values were inferred by the observed date at WLG in 2014 and the average annual decrease rate of 0.02‰ in recent years (Liu et al., 2014).

2.5. Data analysis

Statistical analysis was performed using SPSS software. Variance analysis of CO_2 and CO_{2ff} concentrations were performed by using one-way ANOVA method to evaluate statistically significant difference when $p < 0.05$. Ordinary least square (OLS) technique was used for linear regression analysis.

3. Results and discussion

3.1. Temporal and spatial variations of atmospheric CO_2 concentrations and $\delta^{13}C$ values

Atmospheric CO_2 concentrations and $\delta^{13}C$ values showed obvious seasonal variations during the whole observational period (Fig. 2). The concentrations of atmospheric CO_2 varied from 400.7 ± 3.2 ppm in July 6 to 481.5 ± 23.7 ppm in January, with an average value of 432.8 ± 23.9 ppm, and the median CO_2 concentration was 430.1 ppm. In the winter season (January to March), the CO_2 concentrations ranged from 435.2 ± 11.1 ppm to 481.5 ± 23.7 ppm, with an average value of 456.2 ± 20.9 ppm. This is higher than that in the summer season (June to August), which has a range of 400.7 ± 3.2 ppm to 425.6 ± 3.9 ppm and an average value of 414.2 ± 7.4 ppm, and the peak to peak amplitude of the seasonal fluctuation was 80.8 ppm. Comparing with some regional background sites in China, the amplitude in Xi'an was 19.4 ppm higher than that in Lin'an (Xia et al., 2015) and 22.9 ppm in Shangdianzi (Liu et al., 2014), indicating that urban atmospheric CO_2 concentrations were strongly influenced by anthropogenic activities.

The seasonal variations of the $\delta^{13}C$ values in Xi'an is a reflection of the CO_2 curve (Fig. 2, below), varying from −11.8 ± 0.7‰ to −7.8 ± 0.5‰, with an average value of −9.5 ± 1.2‰ during the observational period. During the winter season, $\delta^{13}C$ ranged from −11.8 ± 0.7‰ to −10.5 ± 0.7‰, and the average value was −11.0 ± 0.4‰; the variations of $\delta^{13}C$ during the summer season ranged from −9.4 ± 0.1‰ to −7.8 ± 0.5‰, with an average value of −8.5 ± 0.6‰, and the amplitude of the seasonal variation is 4.0‰. The seasonal patterns of the CO_2 concentrations and $\delta^{13}C$ values in Xi'an were similar to those in other areas. For example, the CO_2 concentrations in Beijing, China,

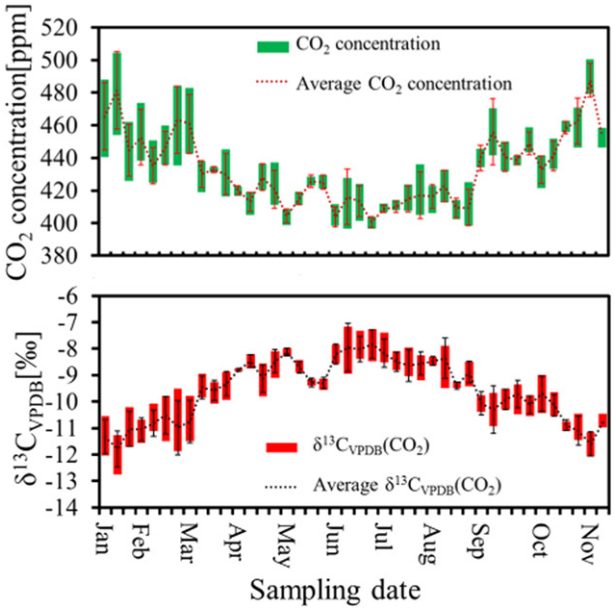

Fig. 2. Temporal variations of the CO_2 concentrations and $\delta^{13}C$ values from 3rd January to 15th November of 2016 ($n = 42$). Vertical bars represent the variation interval of the CO_2 concentrations and $\delta^{13}C$ values; the dotted lines represent the average values of the CO_2 concentrations and $\delta^{13}C$ values. The error bars show the standard deviations of the means across the four sites.

ranged from 372.2 ppm to 635.6 ppm, with an average value of 440.9 ± 37.6 ppm from November 15, 2012, to March 8, 2014 (Pang et al., 2016), and in Bern, Switzerland, the concentration was highest in the winter and lowest in the summer over the period from October 2003 to February 2005 (Sturm et al., 2006); similar results were also found in Los Angeles, USA (Djuricin et al., 2010) and Nagoya, Japan (Wada et al., 2011).

The remarkable differences in the CO_2 concentrations and $\delta^{13}C$ values among the different seasons are mainly due to the changes of local sources and sinks, including the intensity of photosynthesis and respiration, anthropogenic emissions and meteorological conditions (Sturm et al., 2006; Wada et al., 2011). Actually, as a northern Chinese city, there is a special heating period from mid-November to mid-March of the following year in Xi'an, which is called the heating season. In this special period, more fossil fuel consumption causes a massive release of CO_{2ff}. Moreover, because Xi'an is located in Guanzhong plain and sandwiched by the Loess Plateau in the north and the Qinling mountains in the south, air masses were blocked by Qinling mountains when wind blew from northeast direction (Zhao et al., 2015), so the prevailing northwest wind limited the dispersion of urban atmospheric CO_2 in Xi'an during winter. As the heating season ends, atmospheric CO_2 concentration began to decrease rapidly and the value of $\delta^{13}C$ begins to increase. This result supports the assumption that the burning of fossil fuel for heating has a significant contribution to the local excess CO_2 in winter. Coinciding with the increasing of convection of air masses and biogenic activities, the lowest CO_2 concentration and the most enriched $\delta^{13}C$ values occurred in summer.

The spatial variations of the atmospheric CO_2 concentrations and its $\delta^{13}C$ values at all four sites in Xi'an city are shown in Table 1. During the observational period, the CO_2 concentrations in the urban districts were significantly ($p < 0.05$) higher than those of the suburbs in the winter season; the average CO_2 concentration in the urban districts was ~20 ppm higher than that in the suburbs. The considerable difference between the urban and suburban districts became weak, and was not significant ($p > 0.05$) in the spring (April to May). Although the CO_2 concentrations were similar at four sampling sites in the summer, the differences were significant ($p < 0.05$) and the average CO_2 concentration in the suburbs was lower than that in the urban districts

Table 1
The average CO_2 concentrations and $\delta^{13}C$ values with their respective standard deviation in the urban and suburban areas.

Season	A[a]		B[a]		C[b]		D[b]	
	CO_2(ppm)	$\delta^{13}C$(‰)	CO_2(ppm)	$\delta^{13}C$(‰)	CO_2(ppm)	$\delta^{13}C$(‰)	CO_2(ppm)	$\delta^{13}C$(‰)
Winter	466.3 ± 23.7	−11.5 ± 0.7	466.7 ± 21.6	−11.1 ± 0.8	447.2 ± 13.7	−10.5 ± 0.8	444.6 ± 15	−11.1 ± 0.6
Spring	421.9 ± 10.0	−9.2 ± 0.9	423.5 ± 11.7	−9.2 ± 1	416.7 ± 10.9	−9.1 ± 0.7	423.8 ± 12.9	−8.8 ± 0.7
Summer	414.6 ± 8.3	−8.6 ± 0.6	418.1 ± 9.3	−8.4 ± 0.8	412.9 ± 13.1	−8.4 ± 0.7	408.7 ± 9.6	−8.5 ± 0.6
Autumn	452.6 ± 12.8	−10.4 ± 0.7	450 ± 13.2	−10.6 ± 0.6	439.4 ± 4.7	−10 ± 0.4	438.7 ± 11.7	−9.8 ± 0.6
Whole period	436.5 ± 27.2	−9.6 ± 1.3	440.5 ± 25.2	−9.7 ± 1.3	429.7 ± 19.4	−9.4 ± 1.1	426.2 ± 21	−9.3 ± 1.2

[a] Urban site.
[b] Suburban site.

by 5.6 ppm. In the autumn season (September to November), the difference is also significant ($p < 0.05$) and the value differs between the winter and summer by 11.8 ppm. In terms of spatial variations, the observational record showed that the highest CO_2 concentration consistently occurred in urban areas and the lowest occurred in suburban areas. The spatial variations showed the urban CO_2 "dome" effect (Idso et al., 2001) was the most pronounced during the winter season and the least distinct during the summer season in Xi'an. In order to understand the reasons of these changes in different seasons and regions, it is necessary to identify the sources and sinks of urban atmospheric CO_2 and illustrate their spatial and temporal variations.

3.2. Sources of local CO_2 emissions and their spatial and temporal variations

3.2.1. The variations of CO_{2ff} and CO_{2bio} contributions

In this study, air samples collected during winter and summer seasons were used for $\Delta^{14}C$ measurement to quantify the contributions of CO_{2ff} and CO_{2bio} emissions to local atmospheric CO_2. The results showed that $\Delta^{14}C$ values ranged from −126.0 ± 2.8‰ to −7.4 ± 3.6‰ in the winter season and −58.3 ± 2.8‰ to 8.2 ± 3.2‰ in the summer season, with average values of −54.7 ± 31.9‰ and −25.3 ± 17.6‰, respectively. The corresponding CO_{2ff} concentrations were calculated by Eq. (5) which ranged from 68.9 ± 1.4 ppm to 8.2 ± 1.6 ppm with an average concentration of 30.6 ± 15.9 ppm during the winter season, and varied from 29.0 ± 1.3 ppm to 4.2 ± 1.2 ppm in the summer season, with an average concentration of 15.8 ± 7.6 ppm. We interpreted that relatively lower $\Delta^{14}C$ values and higher CO_{2ff} concentrations in the winter season mainly resulted from more fossil fuel consumption.

To compare the differences between the urban and suburban areas, we averaged the two urban samples and two suburban samples to produce weekly average $\Delta^{14}C$ values and CO_{2ff} concentrations, which are presented in Fig. 3(A) and Fig. 3(B), respectively. In the winter season, the $\Delta^{14}C$ value ranged from −118.0 ± 11.3‰ to −28.2 ± 12.9‰, with an average value of −68.6 ± 34.8‰ in the urban areas, which is significantly ($p < 0.05$) lower than that in suburban areas, where the $\Delta^{14}C$ values were in the range of −58.2 ± 24.1‰ ~ −16.5 ± 11.7‰, with an average of −40.8 ± 13.9‰. Conversely, the average CO_{2ff} concentration in the urban areas (37.7 ± 17.8 ppm) was higher than that in the suburban areas (23.5 ± 6.5 ppm) by 14.2 ± 13.2 ppm. Although there were similar trends between urban and suburban areas in the summer season, the average CO_{2ff} concentration in the urban area (18.5 ± 7.3 ppm) was slightly higher than the suburban area (13.5 ± 6.8 ppm) by just 5.0 ± 3.4 ppm. Compared with the differences of the atmospheric CO_2 concentrations in urban and suburban areas (Table 1), the results indicated that the urban CO_2 "dome" effect was mainly caused by CO_{2ff} emissions.

Quantifying the contribution of CO_{2ff} emissions is essential for understanding the spatial and temporal variations of CO_{2ff}. We calculated the excess of CO_2 concentration (CO_{2ex}) by subtracting the background CO_2 concentration from the total CO_2 concentration, and then obtain the contribution of CO_{2ff} to CO_{2ex}. In the winter, the results (Fig. 4) showed the contributions of CO_{2ff} ranged from 51.8% to 78.9% with an average proportion of 61.8 ± 10.6% across the urban areas. Due to more intensive human activities concentrated in urban areas, the contribution of CO_{2ff} emissions is somewhat higher than that in the suburban areas. So there were relatively lower proportions in the suburban areas which varied from 44.2% to 70.4% and with an average of value of 57.4 ± 9.7%. Emissions from biogenic sources account for the remaining fraction and cannot be neglected, because the burning of biomass for cooking and heating is very common in some rural areas surrounding the city. Furthermore, the soil respiration and the decomposition of soil organic matter also release CO_2 back into atmosphere, resulting in biogenic activities played a role of source in local atmospheric CO_2 cycles during the winter season.

Whereas in the summer season, the contributions of CO_{2ff} to CO_{2ex} varied widely (Fig. 4), ranging from 42.3% to >100%. Similar results were also found in Los Angeles, USA (Newman et al., 2013), and Kasprowy, Poland (Zimnoch et al., 2012). These results can be attributed to the intensive photosynthesis during summer season, which removed some amount of CO_2 from local atmosphere. Biosphere occasionally played a role of carbon sink in the case of CO_2 absorbed by photosynthesis is greater than that emitted by respiration. Meanwhile, although CO_{2ff} emissions in winter were much higher than that in summer, biogenic emissions were also more intensive than that in summer (Levin et al., 2003; Zimnoch et al., 2012), resulting in the contributions of CO_{2ff} in the summer (82.5 ± 23.8% in urban areas and 90.0 ± 24.8% in suburban areas) were in fact higher than that in the winter. The higher CO_{2ff} proportions in suburban areas indicate more intensive biogenic activities exist within suburban areas. Additionally, the results also showed the proportions over 100% frequently occurred in late summer when the biomass accumulation reached its maximum.

3.2.2. The variations of $\delta^{13}C$ values of local sources

Although $\Delta^{14}C$ measurements provided quantitative information to assess the emissions from CO_{2ff} and CO_{2bio}, more constraints are needed to recognize the sources of CO_{2ff} further. Here, we used the $\delta^{13}C$ values of local sources ($\delta^{13}C_s$) for this purpose. In this section, $\delta^{13}C_s$ was

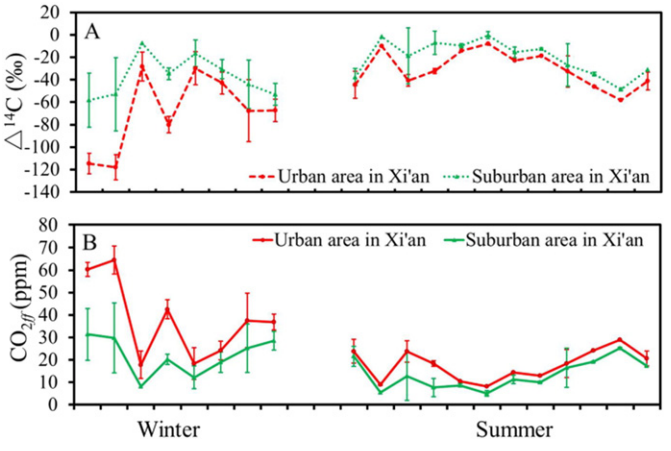

Fig. 3. Average values of $\Delta^{14}CO_2$ (**A**) and CO_{2ff} (**B**) across the winter and summer seasons. The bars indicate the standard deviations of the mean values in urban and suburban areas.

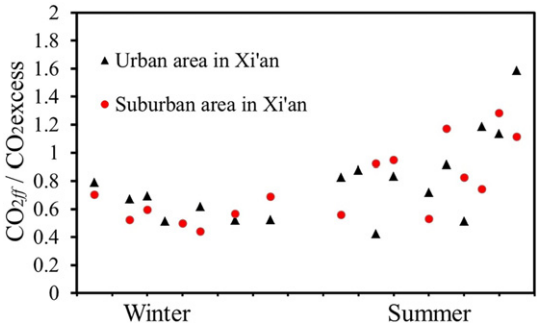

Fig. 4. The proportions of CO_{2ff} in the excess CO_2 during the winter and summer seasons.

determined by using the Miller-Tans method, combined with the results of $\Delta^{14}C$ to recognize the source variations between winter and summer. Generally, $\delta^{13}C_s$ represents the flux-weighted average of more than one sources and/or sinks (Miller and Tans, 2003).

$$\delta^{13}C_s = \delta^{13}C_{ff}F_{ff} + \delta^{13}C_{bio}F_{bio} \quad (7)$$

Here, F is the relative proportions of fossil fuel and biogenic emissions in CO_{2ex}, which were calculated based on the measurements of $\Delta^{14}C$.

The values of $\delta^{13}C_s$ were depleted (−24.9‰) in winter and enriched (−21.9‰) in summer (Fig. 5). As above, $\delta^{13}C_s$ in the winter season is the flux-weighted average of fossil fuel and biogenic emissions, if we adopted isotopic signature of biogenic ($\delta^{13}C_{bio}$) to be −26.2‰ (Pataki et al., 2007), combing with the results of average proportions of fossil fuel emissions in winter, we calculated the $\delta^{13}C$ of fossil fuel emissions ($\delta^{13}C_{ff}$) of −24‰. The value of $\delta^{13}C_{ff}$ in winter season appears very close to the end member of Chinese coal, which has an average value of −23.5‰ (Chen et al., 2012; Tang, 2001). The result suggest that coal burning is the dominate source of fossil fuel emissions in winter. Recently, CO_2 emission inventories for several Chinese cities have been reported (Shan et al., 2017), in the case of Xi'an city, the results showed that coal consumption account for 70% of the total emissions of fossil fuel and industrial processes in 2010. Although some cleaner energy fuels are advocated by the local government in recent years, coal is still the main energy source for heating and electricity generation in Xi'an. Therefore, reducing the share of coal consumption in the energy mix is a hopeful path to control city's CO_2 emissions, especially in the cities of north China, where winter heating is common. Compared with other cities that have similar energy usage patterns, the values of $\delta^{13}C_s$ were more or less consistent with our results. For comparison, in Wroclaw, Poland, the value of $\delta^{13}C_s$ is −25.7‰ and −27.3‰ in two heating season (Górka and Lewicka-Szczebak, 2013). However, some studies in other cities showed more depleted values of $\delta^{13}C_s$ because of the higher proportion of natural gas usage and less coal consumption. For example, $\delta^{13}C_s$ values ranged from −30.0‰ to −37.2‰ in Salt Lake City, USA (Pataki et al., 2003a), and −29.2‰ to −35.7‰ in Chicago, Illinois, USA (Moore and Jacobson, 2015).

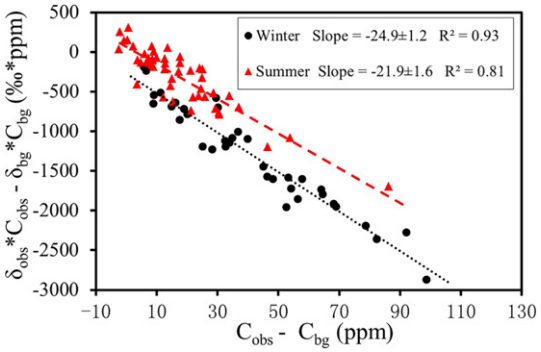

Fig. 5. Miller-Tans plots for the winter and summer in 2016.

In contrast, the enriched $\delta^{13}C_s$ value of −21.9‰ was found in the summer, which lies between the $\delta^{13}C$ values of C4 ecosystem and any other sources. Given that $\delta^{13}C$ end members of fossil fuels lie between coal and natural gas, it is reasonable to predict that the value of $\delta^{13}C_{ff}$ is more depleted than coal (−23.5‰), and thus the value of $\delta^{13}C_{bio}$ should be more enriched than −21.9‰ and more closed to end members of C4-type ecosystem. Actually, as a typical C4 plant, there are large areas of corn planting around Xi'an city and the growth occurs in summer, it seems that the photosynthesis of corn growth period has significant impact on urban carbon cycles. In addition, $\delta^{13}C_s$ value also resembles the soil $\delta^{13}C$ value of −21.7‰ which was found in Yangling, a neighboring city of Xi'an (Tang et al., 2012). We concluded that plant photosynthesis and soil respiration have influenced the atmospheric CO_2 emissions to a certain degree during summer. Similar results have been found in the cities of Dallas (Clark-Thorne and Yapp, 2003) and Wroclaw (Górka and Lewicka-Szczebak, 2013). On the other hand, because seasonal variations of $\delta^{13}C_{bio}$ depending upon the relative abundance of C3/C4 plants and the changes of meteorological conditions (Vardag et al., 2016), using the same $\delta^{13}C_{bio}$ value with winter is unreasonable and the value of $\delta^{13}C_s$ in summer is also fail to support the assumption. Although the measurement of $\Delta^{14}C$ has quantified the contribution of fossil fuel emissions during summer, at this stage, it is difficult to estimate the value $\delta^{13}C_{ff}$ and qualitatively recognize their dominant source of fossil fuel emissions in summer.

4. Conclusions

Based on the measurements of atmospheric CO_2 concentrations and their $\delta^{13}C$ and $\Delta^{14}C$ compositions at four sites in Xi'an city, we present the spatial and temporal variations of urban atmospheric CO_2 and focus on quantifying the contributions of anthropogenic and biogenic emissions. As expected, seasonal variations of the atmospheric CO_2 concentrations and $\delta^{13}C$ values were clearly found. In most cases, atmospheric CO_2 concentrations in the urban areas were significantly ($p < 0.05$) higher than those in the suburban area, especially during winter, when the urban CO_2 "dome" effect was the most pronounced.

The results from the measurements of $\delta^{13}C$ and $\Delta^{14}C$ indicate that the spatial and temporal variations of urban atmospheric CO_2 are influenced by multiple factors, including the changing contribution from anthropogenic emissions in terms of their durations and intensities, and the different intensive of anthropogenic and biogenic activities in different seasons. In particular, CO_{2ff} emissions were the dominant source of local atmospheric CO_2 in the winter season and accounted for approximately 60% of CO_{2ex}, indicating a higher demand of fossil fuel combustion for heating, especially from coal burning. In contrast, the proportions of CO_{2ff} in summer varied largely and occasionally over 100%. The higher average proportions of CO_{2ff} in summer indicate that strong photosynthesis removed part of the CO_2 from local atmosphere, and even played a role of carbon sink in local atmospheric carbon cycles.

Our results suggest that reducing the share of coal consumption is an effective way to mitigate urban atmospheric CO_2 emissions in China. Meanwhile, given that biogenic emissions accounted for nearly 40% of the urban atmospheric CO_2 emissions in the winter and played a significant role in urban carbon cycles in the summer, so the influence of biogenic activities on urban carbon cycles should be taken into account when making mitigation policy and verifying emissions.

Acknowledgments

This work was jointly supported by National Natural Science Foundation of China (NSFC41730108); the MOST special fund for State Key Laboratory of Loess and Quaternary Geology (LQ1301), Chinese Academy of Sciences (Y722011017, Y722011480) and Misitity of Environmental Pretection of Peoples's Republic of China.

References

Ballantyne, A.P., Miller, J.B., Baker, I.T., Tans, P.P., White, J.W.C., 2011. Novel applications of carbon isotopes in atmospheric CO_2: what can atmospheric measurements teach us about processes in the biosphere? Biogeosciences 8, 3093–3106.

Ballantyne, A.P., Andres, R., Houghton, R., Stocker, B.D., Wanninkhof, R., Anderegg, W., Cooper, L.A., DeGrandpre, M., Tans, P.P., Miller, J.B., Alden, C., White, J.W.C., 2015. Audit of the global carbon budget: estimate errors and their impact on uptake uncertainty. Biogeosciences 12, 2565–2584.

Chen, Y., Cai, W., Huang, G., Li, J., zhang, G., 2012. Stable carbon isotope of black carbon from typical emission sources in China. Environ. Sci. 33, 673–678 (in Chinese).

Ciais, P., Rayner, P., Chevallier, F., Bousquet, P., Logan, M., Peylin, P., Ramonet, M., 2010. Atmospheric inversions for estimating CO_2 fluxes: methods and perspectives. Clim. Chang. 103, 69–92.

Clark-Thorne, Yapp, C.J., 2003. Stable carbon isotope constraints on mixing and mass balance of CO_2 in an urban atmosphere: Dallas metropolitan area, Texas, USA. Appl. Geochem. 18, 75–95.

Coplen, T.B., 1996. New guidelines for reporting stable hydrogen, carbon, and oxygen isotope-ratio data. Geochim. Cosmochim. Acta 60, 3359–3360.

Crosson, E.R., 2008. A cavity ring-down analyzer for measuring atmospheric levels of methane, carbon dioxide, and water vapor. Applied Phys. B 92, 403–408.

Dhakal, S., 2009. Urban energy use and carbon emissions from cities in China and policy implications. Energy Policy 37, 4208–4219.

Dhakal, S., 2010. GHG emissions from urbanization and opportunities for urban carbon mitigation. Curr. Opin. Environ. Sustain. 2, 277–283.

Djuricin, S., Pataki, D.E., Xu, X., 2010. A comparison of tracer methods for quantifying CO_2 sources in an urban region. J. Geophys. Res. 115.

Duren, R.M., Miller, C.E., 2012. Measuring the carbon emissions of megacities. Nat. Clim. Chang. 2, 560–562.

Godwin, H., 1962. Half-life of radiocarbon. Nature 195.

Górka, M., Lewicka-Szczebak, D., 2013. One-years spatial and temporal monitoring of concentration and carbon isotopic composition of atmospheric CO_2 in a Wrocław (SW Poland) city area. Appl. Geochem. 35, 7–13.

Graven, H.D., Guilderson, T.P., Keeling, R.F., 2012. Observations of radiocarbon in CO_2 at seven global sampling sites in the Scripps flask network: analysis of spatial gradients and seasonal cycles. J. Geophys. Res.-Atmos. 117, D02303.

Gurney, K.R., Mendoza, D.L., Zhou, Y., Fischer, M.L., Miller, C.C., Geethakumar, S., dela Rue du Can, S., 2009. High resolution fossil fuel combustion CO_2 emission fluxes for the United States. Environ. Sci. Technol. 43.

Hsueh, D.Y., Krakauer, N.Y., Randerson, J.T., Xu, X., Trumbore, S.E., Southon, J.R., 2007. Regional patterns of radiocarbon and fossil fuel-derived CO_2 in surface air across North America. Geophys. Res. Lett. 34.

Idso, C.D., Idso, S.B., Balling Jr., R.C., 2001. An intensive two-week study of an urban CO_2 dome in Phoenix, Arizona, USA. Atmos. Environ. 35, 995–1000.

IEA, 2008. World energy outlook. Head of communication and information. Office International Energy Agency(EIA, Paris.

IPCC, 2006. In: Eggleston, H.S., Buendia, L., Miwa, K., Ngara, T., Tanabe, K. (Eds.), 2006 IPCC Guidelines for National Greenhouse Gas Inventories, Prepared by the National Greenhouse Gas Inventories Programme. Published: IGES, Japan.

Jull, A.J.T., 2007. Radiocarbon dating: AMS method, Encyclopedia of Quaternary Science. Elsevier, Oxford, pp. 2911–2918.

Keeling, C.D., 1958. The concentration and isotopic abundances of atmospheric carbon dioxide in rural areas. Geochim. Cosmochim. Acta 13, 322–334.

Levin, I., Kromer, B., Schmidt, M., Sartorius, H., 2003. A novel approach for independent budgeting of fossil fuel CO_2 over Europe by $^{14}CO_2$ observations. Geophys. Res. Lett. 30.

Liang, S., Zhang, T., 2011. Urban metabolism in China achieving dematerialization and decarbonization in Suzhou. J. Ind. Ecol. 15, 420–434.

Liu, Z., Liang, S., Geng, Y., Xue, B., Xi, F., Pan, Y., Zhang, T., Fujita, T., 2012. Features, trajectories and driving forces for energy-related GHG emissions from Chinese mega cites: the case of Beijing, Tianjin, Shanghai and Chongqing. Energy 37, 245–254.

Liu, L., Zhou, L., Vaughn, B., Miller, J.B., Brand, W.A., Rothe, M., Xia, L., 2014. Background variations of atmospheric CO_2 and carbon-stable isotopes at Waliguan and Shangdianzi stations in China. J. Geophys. Res. Atmos. 119, 5602–5612.

Marland, G., Hamal, K., Jonas, M., 2009. How uncertain are estimates of CO_2 emissions? J. Ind. Ecol. 13, 4–7.

McKaina, K., Wofsya, S.C., Nehrkorn, T., Eluszkiewicz, J., Ehleringer, J.R., Stephensd, B.B., 2012. Assessment of ground-based atmospheric observations for verification of greenhouse gas emissions from an urban region. Proc. Natl. Acad. Sci. U. S. A. 109, 8423–8428.

Miller, J.B., Tans, P.P., 2003. Calculating isotopic fractionation from atmospheric measurements at various scales. Tellus B 55, 207–214.

Miller, J.B., Lehman, S.J., Montzka, S.A., Sweeney, C., Miller, B.R., Karion, A., Wolak, C., Dlugokencky, E.J., Southon, J., Turnbull, J.C., Tans, P.P., 2012. Linking emissions of fossil fuel CO_2 and other anthropogenic trace gases using atmospheric $^{14}CO_2$. J. Geophys. Res. 117.

Moore, J., Jacobson, A.D., 2015. Seasonally varying contributions to urban CO_2 in the Chicago, Illinois, USA region: insights from a high-resolution CO_2 concentration and $\delta^{13}C$ record. Elementa: Science of the Anthropocene. 3.

Necki, J., Schmidt, M., Rozanski, K., Zimnoch, M., Korus, A., Lasa, J.A.N., Graul, R., Levin, I., 2003. Six-year record of atmospheric carbon dioxide and methane at a high-altitude mountain site in Poland. Tellus B 55, 94–104.

Newman, S., Jeong, S., Fischer, M.L., Xu, X., Haman, C.L., Lefer, B., Alvarez, S., Rappenglueck, B., Kort, E.A., Andrews, A.E., Peischl, J., Gurney, K.R., Miller, C.E., Yung, Y.L., 2013. Diurnal tracking of anthropogenic CO_2 emissions in the Los Angeles basin megacity during spring 2010. Atmos. Chem. Phys. 13, 4359–4372.

Newman, S., Xu, X., Gurney, K.R., Hsu, Y.K., Li, K.F., Jiang, X., Keeling, R., Feng, S., O'Keefe, D., Patarasuk, R., Wong, K.W., Rao, P., Fischer, M.L., Yung, Y.L., 2016. Toward consistency between trends in bottom-up CO_2 emissions and top-down atmospheric measurements in the Los Angeles megacity. Atmos. Chem. Phys. 15, 29591–29638.

Niu, Z., Zhou, W., Cheng, P., Wu, S., Lu, X., Xiong, X., Du, H., Fu, Y., 2016. Observations of atmospheric $\Delta^{14}CO_2$ at the global and regional background sites in China: implication for fossil fuel CO_2 inputs. Environ. Sci. Technol. 50, 12122–12128.

Palstra, S.W.L., Karstens, U., Streurman, H.-J., Meijer, H.A.J., 2008. Wine ethanol ^{14}C as a tracer for fossil fuel CO_2 emissions in Europe: measurements and models comparison. J. Geophys. Res. 113.

Pang, J., Wen, X., Sun, X., 2016. Mixing ratio and carbon isotopic composition investigation of atmospheric CO_2 in Beijing, China. Sci. Total Environ. 539, 322–330.

Pataki, D.E., Bowling, D.R., Ehleringer, J.R., 2003a. Seasonal cycle of carbon dioxide and its isotopic composition in an urban atmosphere: anthropogenic and biogenic effects. J. Geophys. Res. 108.

Pataki, D.E., Ehleringer, J.R., Flanagan, L.B., Yakir, D., Bowling, D.R., Still, C.J., Buchmann, N., Kaplan, J.O., Berry, J.A., 2003b. The application and interpretation of Keeling plots in terrestrial carbon cycle research. Glob. Biogeochem. Cycles 17.

Pataki, D.E., Xu, T., Luo, Y.Q., Ehleringer, J.R., 2007. Inferring biogenic and anthropogenic carbon dioxide sources across an urban to rural gradient. Oecologia 152, 307–322.

Riley, W.J., Hsueh, D.Y., Randerson, J.T., Fischer, M.L., Hatch, J.G., Pataki, D.E., Wang, W., Goulden, M.L., 2008. Where do fossil fuel carbon dioxide emissions from California go? An analysis based on radiocarbon observations and an atmospheric transport model. J. Geophys. Res. 113.

Seto, K.C., Dhakal, S., Bigio, A., Blanco, H., Delgado, G.C., Dewar, D., Huang, L., Inaba, A., Kansal, A., Lwasa, S., McMahon, J.E., Müller, D.B., Murakami, J., Nagendra, H., Ramaswami, A., 2014. Human Settlements, Infrastructure and Spatial Planning. In: Edenhofer, O., Pichs-Madruga, R., Sokona, Y., Farahani, E., Kadner, S., Seyboth, K., Adler, A., Baum, I., Brunner, S., Eickemeier, P., Kriemann, B., Savolainen, J., Schlömer, S., von Stechow, C., Zwickel, T., Minx, J.C. (Eds.), Climate Change 2014: Mitigation of Climate Change. Contribution of Working Group III to the Fifth Assessment Report of the Intergovernmental Panel on Climate Change. Cambridge University Press, Cambridge, United Kingdom and New York, NY, USA.

Shan, Y., Guan, D., Liu, J., Mi, Z., Liu, Z., Liu, J., Schroeder, H., Cai, B., Chen, Y., Shao, S., Zhang, Q., 2017. Methodology and applications of city level CO_2 emission accounts in China. J. Clean. Prod. 161, 1215–1225.

Slota, P.J., Jull, A.J.T., Linick, T.W., Toolin, L.J., 1987. Preparation of small samples for ^{14}C accelerator targets by catalytic reduction of CO. Radiocarbon 29, 303–306.

Stuiver, M., Polach, H.A., 1977. Discussion reporting of ^{14}C data. Radiocarbon 19, 355–363.

Sturm, M., Leuenberger, F., Valentino, L., Lehmann, B., Ihly, B., 2006. Measurements of CO_2, its stable isotopes, O_2/N_2, and ^{222}Rn at Bern,Switzerland. Atmos. Chem. Phys. 6, 1991–2004.

Suess, H.E., 1955. Radiocarbon concentration in modern wood. Science 122, 415–417.

Tang, G., 2001. $\delta^{13}C$ Characteristics of Carboniferous Coal in North China and Its Palaeogeographic Implications. Political Scholars Anthology of Peking University. Peking University, Peking (in Chinese).

Tang, X., Ellert, B.H., Hao, X., Ma, Y., Nakonechny, E., Li, J., 2012. Temporal changes in soil organic carbon contents and $\delta^{13}C$ values under long-term maize–wheat rotation systems with various soil and climate conditions. Geoderma 183-184, 67–73.

Tans, P., Wallace, D., 1999. Carbon cycle research after Kyoto. Tellus Ser. B Chem. Phys. Meteorol. 51, 562–571.

Turnbull, J.C., Miller, J.B., Lehman, S.J., Tans, P.P., Sparks, R.J., Southon, J., 2006. Comparison of $^{14}CO_2$, CO, and SF_6 as tracers for recently added fossil fuel CO_2 in the atmosphere and implications for biological CO_2 exchange. Geophys. Res. Lett. 33.

Turnbull, J., Rayner, P., Miller, J., Naegler, T., Ciais, P., Cozic, A., 2009. On the use of $^{14}CO_2$ as a tracer for fossil fuel CO_2: quantifying uncertainties using an atmospheric transport model. J. Geophys. Res. 114, D22302.

Vardag, S.N., Hammer, S., Levin, I., 2016. Evaluation of 4 years of continuous $\delta^{13}C(CO_2)$ data using a moving Keeling plot method. Biogeosciences 13, 4237–4251.

Wada, R., Pearce, J.K., Nakayama, T., Matsumi, Y., Hiyama, T., Inoue, G., Shibata, T., 2011. Observation of carbon and oxygen isotopic compositions of CO_2 at an urban site in Nagoya using mid-IR laser absorption spectroscopy. Atmos. Environ. 45, 1168–1174.

Widory, D., Javoy, M., 2003. The carbon isotope composition of atmospheric CO_2 in Paris. Earth Planet. Sci. Lett. 215, 289–298.

WMO, 2016. Greenhouse Gas Bulletin:The State of Greenhouse Gases in the Atmosphere Based on Global Observations through 2015.

Xia, L., Zhou, L., Tans, P.P., Liu, L., Zhang, G., Wang, H., Luan, T., 2015. Atmospheric CO_2 and its $\delta^{13}C$ measurements from flask sampling at Lin'an regional background station in China. Atmos. Environ. 117, 220–226.

Zhao, S., Tie, X., Cao, J., Zhang, Q., 2015. Impacts of mountains on black carbon aerosol under different synoptic meteorology conditions in the Guanzhong region, China. Atmos. Res. 164–165, 286–296.

Zhou, W., Zhao, X., Xuefeng, L., Lin, L., Zhengkun, W., Peng, C., Wengnian, Z., Chunhai, H., 2006. The 3MV multi-element AMS in Xi'an, China: unique features and preliminary tests. Radiocarbon 48, 285–293.

Zhou, W., Wu, S., Huo, W., Xiong, X., Cheng, P., Lu, X., Niu, Z., 2014. Tracing fossil fuel CO_2 using $\Delta^{14}C$ in Xi'an City, China. Atmos. Environ. 94, 538–545.

Zimnoch, M., Jelen, D., Galkowski, M., Kuc, T., Necki, J., Chmura, L., Gorczyca, Z., Jasek, A., Rozanski, K., 2012. Partitioning of atmospheric carbon dioxide over Central Europe: insights from combined measurements of CO_2 mixing ratios and their carbon isotope composition. Isot. Environ. Health Stud. 48, 421–433.

Zobitz, J.M., Keener, J.P., Schnyder, H., Bowling, D.R., 2006. Sensitivity analysis and quantification of uncertainty for isotopic mixing relationships in carbon cycle research. Agric. For. Meteorol. 136, 56–75.